Spectroscopic data for atomic tungsten transitions of interest in fusion plasma research

P Quinet†‡, P Palmeri† and É Biémont†‡

† Astrophysique et Spectroscopie, Université de Mons – UMONS, B-7000 Mons, Belgium

‡ IPNAS, Université de Liège, B15 Sart Tilman, B-4000 Liège, Belgium

E-mail: quinet@umons.ac.be

Abstract. Transition probabilities for W I lines of potential interest for fusion plasma diagnostics are reported in the present paper. They have been obtained using the relativistic Hartree-Fock approach including core-polarization effects. The accuracy of the results has been assessed through comparison between two different physical models and through detailed comparison with available experimental lifetimes and transition probabilities. These results represent the first complete set of spectroscopic parameters computed for the very complex tungsten atomic system. The new data are expected to be useful for plasma modeling in fusion reactors such as *ITER*.

Submitted to : *J. Phys. B: At. Mol. Opt. Phys.*

1. Introduction

Reliable spectroscopic parameters in tungsten atom are of fundamental importance for the study and modeling of plasmas in fusion reactors. Indeed, tungsten is a very attractive element to be used as a plasma facing material in Tokamak devices because of its high melting point (3410°C) and thermal conductivity, its low tritium retention and erosion rate under plasma loading (see e.g. Federici *et al* 2001, Pospieszczyk 2006). Some years ago, several experiments were carried out in ASDEX Upgrade device to prove the suitability of W as a divertor target material under the conditions of a high density and low temperature divertor (Naujoks *et al* 1996). The *International Thermonuclear Experimental Reactor* (*ITER*) will be the next step experimental fusion device which will use tungsten, together with beryllium and carbon-fiber reinforced composite, as plasma facing materials. The main disadvantage of tungsten in these conditions is the large radiative loss due to plasma contamination and related to its high radiative efficiency.

In fusion reactors, tungsten will be sputtered from the plasma wall as a neutral element and the intensity of the well-known W I emission line at 400.8753 nm may be used to estimate tungsten influx (Skinner 2008). Unfortunately, a complication arises from the fact that there exists a coincident W II line at 400.8751 nm.

The determination of the tungsten influx rate to the core plasma will depend on a calculation of transport from the wall surface through the scrape-off layer. Consequently the identification of emission lines from the lowest ionization stages of tungsten, including the neutral atom, will greatly aid modeling of the plasma edge and scrape-off layer transport and facilitate the analysis of net tungsten influx rates.

Up to now, transition probabilities in neutral tungsten were essentially obtained experimentally by Den Hartog *et al* (1987) and Kling and Kock (1999) for a selection of lines depopulating energy levels for which radiative lifetimes had been measured in laboratory. The aim of the present paper is to extend the set of available transition rates for W I lines not considered so far. The method used is based on the relativistic Hartree-Fock (HFR) approach including core-polarization corrections. This work is an extension of similar investigations carried out in W II and W III ions (Nilsson *et al* 2008, Palmeri *et al* 2008). Furthermore, let us note that critically evaluated transition rates available in the literature for allowed electric dipole transitions together with a new set of computed A-values for forbidden lines were reported in our recent paper (Quinet *et al* 2010) for W I, W II and W III.

2. Available spectroscopic data in W I

2.1. Wavelengths and energy levels

Wavelengths of all the transitions observed in the W I spectrum, and energy levels derived from these wavelengths, were compiled by Kramida and Shirai (2006) who critically evaluated the data published previously by Laun and Corliss (1968), Shadmi and Caspi (1968), Corliss (1969), Wyart (1978), Martin *et al* (1978) and Campbell-

Miller and Simard (1996). Of the 6800 arc lines listed by Kramida and Shirai (2006) in the spectral region 200 – 1048 nm, about 5500 were classified using 101 even-parity levels in the range 0 – 56833 cm^{-1} and 365 odd-parity levels in the range 19389 – 63533 cm^{-1}. Whereas the 70 lowest even-parity levels belonging to the $5d^46s^2$ and $5d^56s$ configurations had been studied parametrically by Shadmi and Caspi (1968), the system of odd-parity levels had not received adequate interpretation until the recent investigation due to Wyart (2010). In this latter work, a comprehensive study of all odd-parity levels with energies lower than 45000 cm^{-1} was performed using the HFR method supported by the semi-empirical fitting of radial parameters corresponding to the $5d^46s6p$, $5d^56p$ and $5d^36s^26p$ configurations. This led to the classification of the 141 lowest odd-parity levels including two new levels located at 29823.09 cm^{-1} ($J = 0$) and 37451.33 cm^{-1} ($J = 6$) that were the only odd-parity levels still missing below 43000 cm^{-1}.

2.2. Radiative lifetimes and transition probabilities

Transition probabilities in neutral tungsten were first determined experimentally by Corliss and Bozman (1962) but their arc measurements later on were recognized to be affected by large systematic errors. These results were supplemented by the relative measurements of Clawson and Miller (1973) and by the absolute measurements of Obbarius and Kock (1982). In the latter case, a stabilized arc, operated in argon, was used for measuring oscillator strengths for 43 W I lines in the wavelength range 240–560 nm. The accuracy of the relative data of Clawson and Miller was estimated to range between 6 and 50% while the f-values measured by Obbarius and Kock were reported with uncertainties from 10 to 36%.

The first experimental measurements of radiative lifetimes in W I were performed by Duquette *et al* (1981) who used time-resolved laser-induced fluorescence (TR-LIF) and a hollow cathode effusive atomic beam source for lifetime determination of 15 levels belonging to the $5d^46s6p$ and $5d^56p$ configurations with an accuracy of ±5%. Kwiatkowski *et al* (1982) reported lifetimes for 13 energy levels in the configurations $(5d+6s)^56p$. These measurements were based on the observation of the reemitted fluorescence with single-photon-counting technique after a selective excitation of an atomic beam by a pulsed dye laser. Some radiative lifetimes of W I excited states were also published by Plekhotkin and Verolainen (1985).

The TR-LIF technique was also used by Schnabel and Kock (1997) to measure radiative lifetimes for 47 W I levels in the energy range 27800 to 48200 cm^{-1} with an accuracy of 2 – 7%. These results agree within the mutual uncertainties with the measurements (accurate to ±5%) of Den Hartog *et al* (1987) (3 lifetimes common to both works). The lifetimes of Kwiatkowski *et al* agree within 7 % with those of Den Hartog *et al* (1987) (13 levels in common), the latter work including remeasurements of the values published by Duquette *et al* (1981).

The most extensive sets of experimental transition probabilities in neutral tungsten

were reported by Den Hartog *et al* (1987) and Kling and Kock (1999) who measured branching fractions (BF) on high resolution Fourier transform spectra and were able to deduce absolute transition probabilities for a set of 572 lines covering the wavelength range 225–1035 nm and involving excited energy levels up to 46932 cm^{-1}. The typical uncertainties of A-values for the most intense lines ($A \geq 10^6$ s^{-1}) were estimated to range between 5 and 20% and between 7 and 9% for the former and the latter authors, respectively. The lifetimes used in these two papers were those of Den Hartog *et al* (1987) and of Schnabel and Kock (1997), respectively. As the work of Kling and Kock (1999) was focused on higher-lying levels than that of Den Hartog *et al* (1987), the overlap of the two works is small. In fact BFs were measured for only 19 lines in common. The agreement is within a few (< 7) % for the most intense transitions (BF > 20 %), larger discrepancies appearing (as expected) for some weaker lines.

More recently, Wyart (2010) used the HFR method of Cowan (1981) for generating a set of computed transition probabilities for a selection of 70 lines depopulating 12 odd-parity levels. Although obtained by considering a rather simple physical model (including only $5d^46s^2 + 5d^56s + 5d^6$ and $5d^46s6p + 5d^56p + 5d^36s^26p$ for even and odd parities, respectively), a fair qualitative agreement was noted between these calculated gA-values and the observed line intensities reported in the compilation of Kramida and Shirai (2006).

3. Computational method

The theoretical method considered for computing the decay rates in W I is the well established HFR approach originally developed by Cowan (1981) in which we have included core-polarization effects (see e.g. Quinet *et al* 1999). Two sets of calculations were performed in the present work. In the first one (Model A), the following configurations were explicitly included : $5d^46s^2$, $5d^56s$, $5d^57s$, $5d^6$, $5d^46s7s$, $5d^46s6d$, $5d^56d$, $5d^46p^2$, $5d^46d^2$, $5d^36s6p^2$, $5d^26s^26p^2$ (even parity) and $5d^46s6p$, $5d^46s7p$, $5d^56p$, $5d^57p$, $5d^46s5f$, $5d^55f$, $5d^36s^26p$, $5d^36p^3$, $5d^26s6p^3$ (odd parity). For the dipole polarizability, α_d, we have adopted the value of 4.59 a_0^3 (Fraga *et al* 1976) corresponding to the ytterbium-like W^{4+} ionic core. The cut-off radius, r_c, was chosen equal to 1.99 a_0 which corresponds to the HFR average value $<r>$ for the outermost 5d core orbital. In the second physical model (Model B), configuration interaction was considered by including the same configurations as those considered in Model A except $5d^26s^26p$ (even parity) and $5d^26s6p^3$ (odd parity). In this case, the core-polarization effects corresponding to a lutecium-like ionic core were considered using the dipole polarizability of W^{3+}, i.e. $\alpha_d = 6.88$ a_0^3 (Fraga *et al* 1976) and the same value as the one used in Model A for the cut-off radius, i.e. $r_c = 1.99$ a_0. The only difference between both models thus lies in the way core-valence interactions are taken into account. By assuming an ionic core with 70 electrons in the core polarization potential and opening the 5d subshell up to $5d^2$, these interactions are considered more explicitly in Model A than in Model B where a slightly bigger ionic core containing 71 electrons is incorporated in the potential.

In each of these approaches, the final wavefunctions were obtained by a parametric fit of the calculated energy levels to the experimental ones. All the even experimental levels compiled by Kramida and Shirai (2006) for $5d^46s^2$ and $5d^56s$ configurations were fitted using, as adjustable parameters, the average energies (E_{av}), the Slater radial integrals (F^k, G^k, R^k), the spin-orbit parameters (ζ_{nl}) and the effective interaction parameters (α, β). In the case of odd-parity levels, only the lowest experimental values ($E < 45000$ cm^{-1}) published by Wyart (2010) were included in the fitting procedure using the E_{av}, F^k, G^k, R^k, ζ_{nl} and α parameters of the $5d^46s6p$, $5d^56p$ and $5d^36s^26p$ configurations as variable parameters. The mean deviation, $|\Delta E| = |E_{exp} - E_{calc}|$, obtained when fitting the even-parity levels (70 levels) was found to be equal to almost the same value in both models ($|\Delta E_A| = 57$ cm^{-1} and $|\Delta E_B| = 59$ cm^{-1}) while this parameter was slightly increased for odd-parity levels (141 levels) when going from model A to model B ($|\Delta E_A| = 64$ cm^{-1} and $|\Delta E_B| = 73$ cm^{-1}).

4. Results and discussion

The calculated energy levels and Landé g-factors are compared with experiment in Tables 1 and 2 for even and odd parities, respectively. A detailed knowledge of the Landé factors is important to analyse the atomic spectra when an external magnetic field is applied. It can also provide us with useful information regarding the spin-orbit interaction and, consequently, the coupling schemes encountered in atoms. Moreover, the g-factor is helpful for the assignement of the energy levels in term analysis and allows us to get a deeper insight into the properties of atomic states in heavy elements such as W I, for which this parameter was still unknown for many levels. When looking at Tables 1 and 2, a very good overall agreement is observed between the theoretical results (using both models A and B) and the available experimental Landé factors. The present determination of g-values in neutral tungsten is an extension of a similar work recently performed for some atoms and ions along the sixth row of the periodic table (Biémont *et al* 2010).

Calculated radiative lifetimes obtained in the present work using model A, τ_A, and model B, τ_B, are compared to the available experimental measurements in Table 2 for odd-parity levels below 45000 cm^{-1}. This comparison is illustrated in Figure 1 showing the ratio τ_{exp}/τ_{calc} as a function of the energy. It is seen that the overall agreement between experimental lifetimes and calculated ones is rather similar whatever the physical model used, the mean ratio τ_{exp}/τ_{calc} being found to be equal to 1.12 ± 0.40 and 1.02 ± 0.38 in the cases of models A and B, respectively. We also note that the most important discrepancies with experimental measurements appear for some levels below 30000 cm^{-1} and above 40000 cm^{-1}. This can be explained by the fact that the former levels, characterized by long lifetimes ($\tau_{exp} > 500$ ns), are depopulated by weak transitions for which the computed line strengths were found to be affected by important cancellation effects while the levels above 40000 cm^{-1} were found to be very strongly mixed, their eigenvector purities rarely exceeding 15%. This is illustrated in

Figure 2 showing the LS-coupling purities obtained using theoretical model A for all the odd-parity levels below 45000 cm^{-1}.

The calculated transition probabilities, gA, obtained in the present work using both models A and B are reported in Table 3 alongside the lower (even) and upper (odd) experimental energy levels of the transition and the air wavelengths in nm. These wavelengths were taken from the compilation due to Kramida and Shirai (2006). Only transitions with calculated gA-values (model A) greater than 5×10^7 s^{-1} are listed in Table 3. The complete table is available in our DESIRE database at the following address : http://w3.umons.ac.be/∼astro/desire.shtml. Experimental transition probabilities, when available, are also given in Table 3 for comparison. These values were obtained by Den Hartog *et al* (1987) and Kling and Kock (1999). When looking at this table, we note that the general agreement between theoretical results and experimental ones is better in the case of model A than in the case of model B, the mean ratio gA_{exp}/gA_{calc} being found to be equal to 1.10 ± 0.74 and 1.36 ± 1.32, respectively, if we except the line at 248.0130 nm for which the calculated transition probability is affected by large cancellation effects in model B. When compared with experimental gA-values, results of calculation B also seem to show a larger systematic underestimate and a larger scattering than those deduced from calculation A. This is probably due to the fact that core-valence interactions are better represented in model A than in model B. Consequently, it is expected that transition probabilities obtained in the present work using model A are more reliable than those computed with model B. This statement should however be checked on a firmer basis by new experimental measurements.

It is also worth noting that a better overall agreement is observed when comparing the calculations with the experimental transition probabilities measured by Den Hartog *et al* (1987) than with those reported by Kling and Kock (1999), as shown in Figures 3 and 4, a larger scattering being observed in the latter case even for intense transitions. This is probably due to the fact that the work of Kling and Kock was focused on higher-lying levels of which most are characterized by very strong mixings in the wavefunction expansions, as already mentioned above for levels with $E > 40000$ cm^{-1}.

5. Conclusion

A new set of computed transition probabilities for neutral tungsten lines is reported in the present work. The accuracy of these results was assessed through detailed comparisons between two different HFR models and available experimental data. These data represent the first complete set of spectroscopic parameters computed for the very complex W I atomic structure. It is expected that the results will provide plasma physicists with some of the data they need for spectroscopic diagnostics and modeling of fusion plasmas magnetically confined in reactors where tungsten is expected to be used as a facing material.

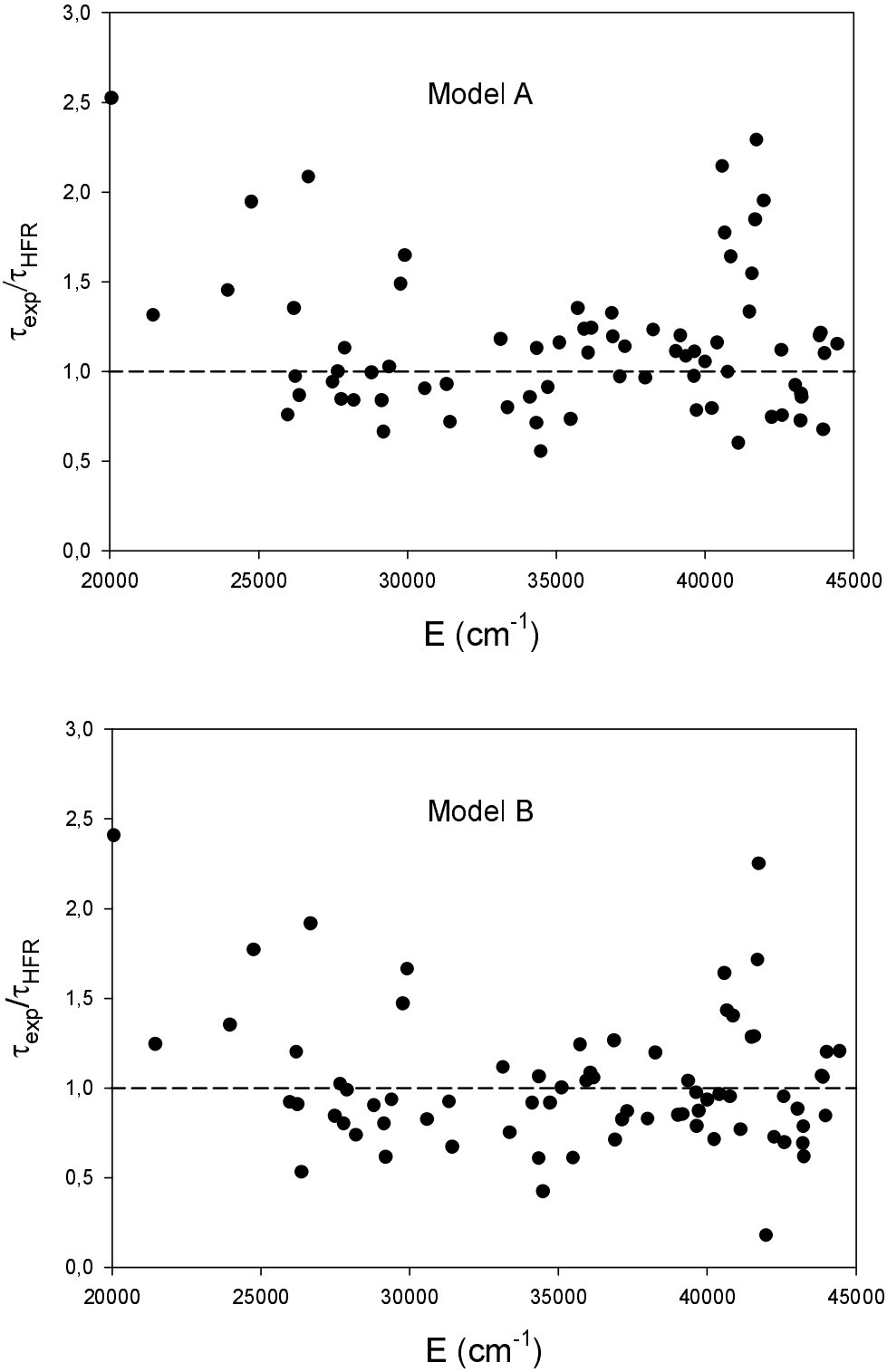

Figure 1. Comparison between calculated radiative lifetimes as obtained in the present work using both physical models (A and B) and experimental values published by Den Hartog *et al* (1987) and Schnabel and Kock (1997)

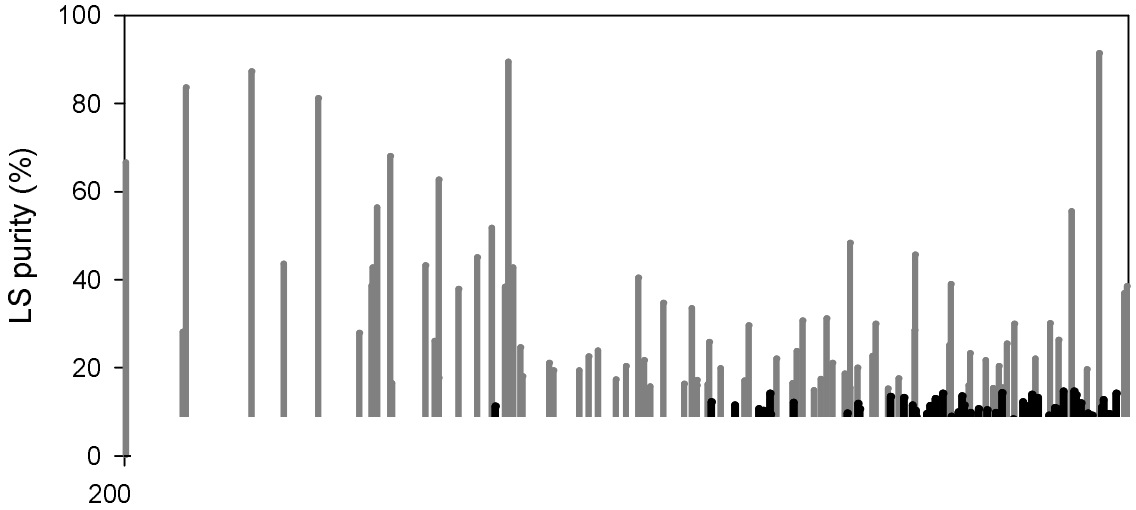

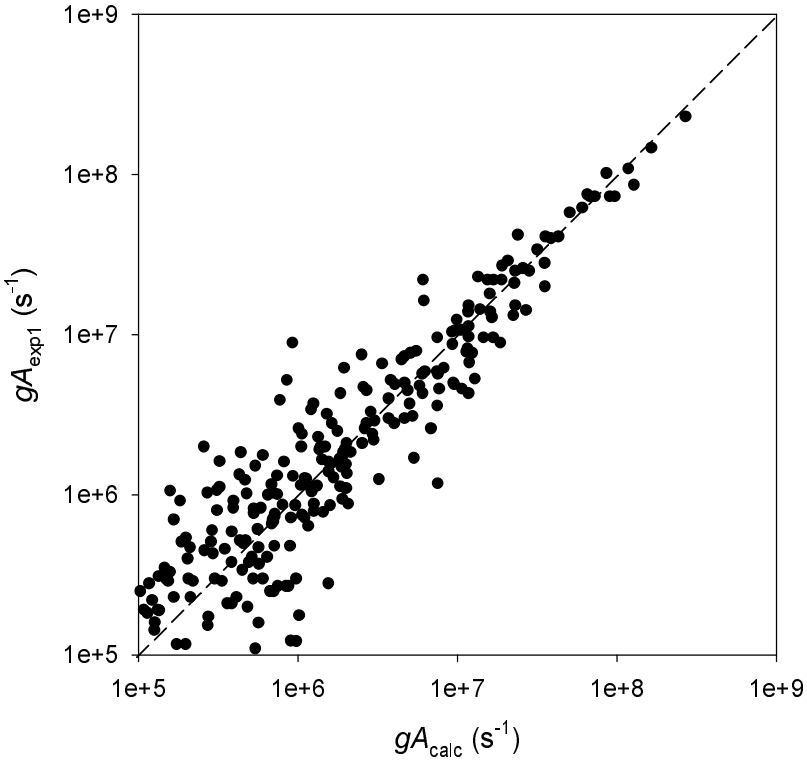

Figure 3. Comparison between calculated transition probabilities (gA_{calc}) as obtained in the present work (Model A) and experimental values (gA_{exp1}) published by Den Hartog *et al* (1987)

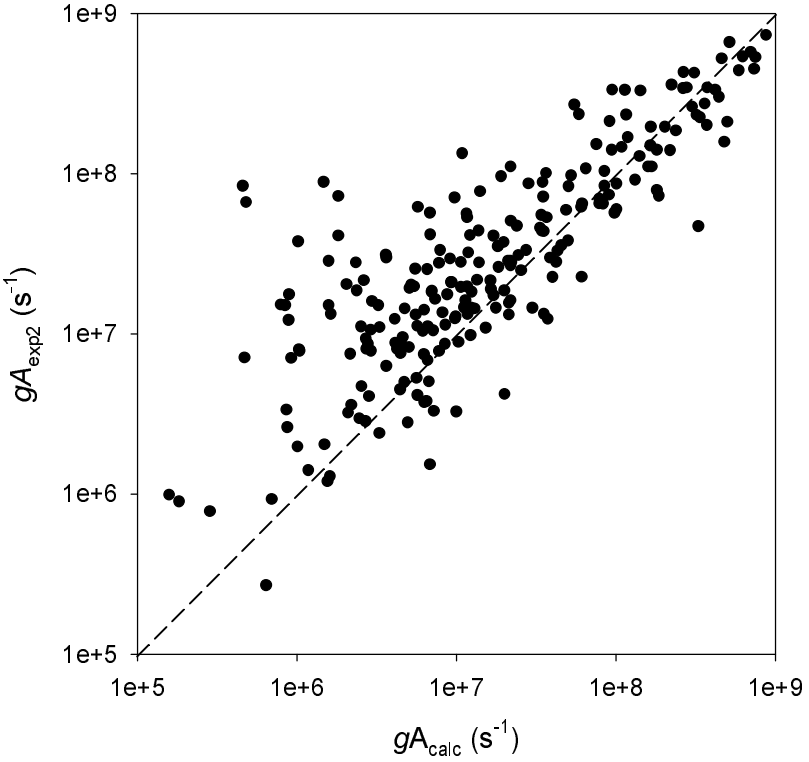

Figure 4. Comparison between calculated transition probabilities (gA_{calc}) as obtained in the present work (Model A) and experimental values (gA_{exp2}) published by Kling and Kock (1999)

Acknowledgments. PQ, PP and EB are, respectively Senior Research Associate, Research Associate and Research Director of the FRS-FNRS. Financial support from the ADAS-EU project is acknowledged.

References

Biémont E, Palmeri P, Quinet P 2010 *J. Phys. B : At. Mol. Opt. Phys.* **43** 074010
Campbell-Miller M D, Simard B 1996 *J. Opt. Soc. Am. B* **13** 2115
Clawson J E, Miller M H 1973 *J. Opt. Soc. Am.* **63** 1598
Corliss C H 1969 *J. Res. Nat. Bur. Stand. Sect. A* **73** 277
Corliss C H, Bozman W R 1962 *Nat. Bur. Stand. Monograph* **53** (Washington DC : US Government Printing Office)
Cowan R D 1981 *The Theory of Atomic Structure and Spectra* (Berkeley, CA : University of California Press)
Den Hartog E A, Duquette D W, Lawler J E 1987 *J. Opt. Soc. Am. B* **4** 48
Duquette D W, Salih S, Lawler J E 1981 *Phys. Rev. A* **24** 2847
Ekberg J O, Kling R, Mende W 2000 *Phys. Scr.* **61** 146
Federici G *et al* 2001 *Nucl. Fus.* **41** 1967
Fraga S, Karwowski J, Saxena K M S 1976 *Handbook of Atomic Data* (Amsterdam : Elsevier)
Kling R, Kock M 1999 *J. Quant. Spectrosc. Radiat. Transfer* **62** 129
Kramida A E, Shirai T 2006 *J. Phys. Chem. Ref. Data* **35** 423
Kwiatkowski M, Micali G, Werner K, Schmidt M, Zimmermann P 1982 *Z. Phys. A* **304** 197
Laun D D, Corliss C H 1968 *J. Res. Nat. Bur. Stand. Sect. A* **72** 609

Martin W C, Zalubas R, Hagan L 1978 *Nat. Bur. Stand. Monograph* **60** (Washington DC : US Department of Commerce)

Naujoks D, Asmussen K, Bessenrodt-Weberpals M, Deschka S, Dux R, Engelhardt W, Field A R, Fussmann G, Fuchs J C, Garcia-Rosales C, Hirsch S, Ignacz P, Lieder G, Mast K F, Neu R, Radtke R, Roth J, Wenzel U, ASDEX Upgrade Team 1996 *Nuclear Fusion* **36** 671

Nilsson H, Engström L, Lundberg H, Palmeri P, Fivet V, Quinet P, Biémont É 2008 *Eur. Phys. J. D* **49** 13

Obbarius H U, Kock M 1982 *J. Phys. B* **15** 527

Palmeri P, Quinet P, Fivet V, Biémont E, Nilsson H, Engström L, Lundberg H 2008 *Phys. Scr.* **78** 015304

Plekhotkin G A, Verolainen Ya F 1985 *Opt. Spectrosc.* **58** 447

Pospieszczyk A 2006 *Nuclear Fusion Research* (Berlin Heidelberg : Springer)

Quinet P, Palmeri P, Biémont E, McCurdy M M, Rieger G, Pinnington E H, Wickliffe M E, Lawler J E 1999 *Mon. Not. R. Astr. Soc.* **307** 934

Quinet P, Vinogradoff V, Palmeri P, Biémont E 2010 *J. Phys. B : At. Mol. Opt. Phys.* **43** 144003

Schnabel R, Kock M 1997 *Z. Phys. D* **41** 31

Shadmi Y, Caspi E 1968 *J. Res. Nat. Bur. Stand. Sect. A* **72** 757

Skinner H C 2008 *Can. J. Phys.* **86** 285

Wyart J-F 1978 *Phys. Scr.* **18** 87

Wyart J-F 2010 *J. Phys. B : At. Mol. Opt. Phys.* **43** 074018

Table 1. Experimental and calculated energies, Landé factors and radiative lifetimes for W I even-parity levels below 37500 cm^{-1}.

J	$E_{exp}{}^a$ (cm^{-1})	$E_A{}^b$ (cm^{-1})	$\Delta E_A{}^c$ (cm^{-1})	$E_B{}^d$ (cm^{-1})	$\Delta E_B{}^e$ (cm^{-1})	$g_{exp}{}^a$	$g_A{}^b$	$g_B{}^d$
0	0.00	-88	88	-90	90			
1	1670.29	1697	-27	1697	-27	1.51	1.50	1.50
3	2951.29	2893	58	2886	65	1.98	1.98	1.98
2	3525.53	3381	-56	3381	-56	1.48	1.49	1.49
3	4830.00	4838	-8	4838	-8	1.50	1.48	1.48
4	6219.33	6118	101	6117	102	1.49	1.45	1.45
0	9528.06	9524	4	9523	5			
4	12161.96	12161	1	12156	6	0.99	0.99	0.99
1	13307.10	13412	-105	13431	-124	1.32	1.29	1.29
3	13348.56	13417	-68	13410	-61	0.92	0.94	0.94
2	13777.71	13699	79	13697	81	1.09	1.07	1.07
2	14976.18	15033	-57	15050	-74	1.06	0.96	0.96
5	15069.93	15094	-24	15094	-24	1.05	1.10	1.10
3	15460.01	15400	60	15394	66	1.17	1.26	1.26
4	16431.31	16526	-95	16514	-83	1.02	1.01	1.01
6	17008.50	16988	21	16996	13	1.4	1.14	1.14
4	17107.01	17043	64	17044	63	1.19	1.12	1.12
3	17701.18	17709	-8	17711	-10	1.02	1.03	1.03
1	18082.83	18090	-7	18082	1	0.7	0.79	0.79
2	18116.84	18171	-54	18165	-48	1.08	1.42	1.52
2	18280.48	18308	-28	18313	-33	1.43	1.06	0.97
3	18974.51	19009	-34	19009	-34	1.06	1.07	1.08
2	19253.56	19291	-37	19304	-50	1.18	1.23	1.24
4	19256.24	19293	-37	19302	-46	1.20	1.18	1.18
5	19535.01	19623	-88	19622	-87	1.21	1.15	1.14
6	19648.54	19657	-8	19665	-16	1.32	1.32	1.32
5	19826.04	19756	70	19762	64	1.20	1.26	1.26
3	19827.68	19812	16	19808	20	1.28	1.42	1.42
0	20174.20	20084	90	20052	122			
1	20427.84	20429	-1	20423	5	2.1	2.11	2.11
2	20983.02	21036	-53	21041	-58		1.57	1.57
4	22476.68	22464	13	22468	9	1.48	1.39	1.38
0	22773.78	22819	-45	22819	-45			
4	22852.80	22787	66	22772	81	1.2	1.11	1.11
1	23455.02	23490	-35	23488	-33		1.72	1.72
6	23484.78	23444	41	23449	36		1.03	1.03
3	23930.08	23864	66	23861	69	1.4	1.49	1.49
2	23982.80	23981	2	23978	5		1.56	1.56
3	24610.88	24628	-17	24633	-22		1.03	1.03
2	24789.66	24841	-51	24860	-70		1.14	1.14
2	26861.64	26859	3	26865	-3		0.98	0.98
4	27213.82	27112	102	27122	92		1.25	1.25
1	27670.48	27816	-146	27809	-139		0.15	0.16
5	27849.80	27806	44	27804	46		0.92	0.92
2	28204.20	28292	-88	28289	-85		1.03	1.03

Table 1. Continued.

J	E_{exp}[a] (cm^{-1})	E_A[b] (cm^{-1})	ΔE_A[c] (cm^{-1})	E_B[d] (cm^{-1})	ΔE_B[e] (cm^{-1})	g_{exp}[a]	g_A[b]	g_B[d]
5	28233.44	28072	161	28080	153		1.35	1.35
3	28291.88	28229	63	28236	56		1.11	1.11
3	28347.60	28344	4	28336	12		1.15	1.16
6	28392.70	28475	-82	28472	-79		1.05	1.05
1	28720.88	28801	-80	28808	-87		1.44	1.44
2	28898.96	28814	85	28835	64		1.15	1.14
0		29036		29040				
3	29430.50	29520	-89	29519	-88		1.00	1.01
7	29460.98	29575	-114	29574	-113		1.14	1.14
4	29479.32	29517	-38	29515	-36		1.28	1.28
4	29853.66	29837	17	29837	17		1.03	1.03
2	30374.20	30275	99	30242	132		1.12	1.12
2	31077.80	31180	-102	31190	-112		1.06	1.06
5	31389.08	31300	89	31305	84		1.12	1.12
4	32135.94	32086	50	32081	55		1.06	1.06
3	32217.91	32236	-18	32226	-8		1.04	1.04
1	32378.40	32433	-55	32436	-58		0.49	0.49
3	32826.63	32797	30	32806	21		1.01	1.00
1		33035		33008			0.88	0.88
5	33201.61	33210	-8	33201	1		1.14	1.14
6	33291.80	33220	72	33211	81		1.07	1.07
4	33569.53	33589	-20	33580	-10		1.01	1.01
3	33952.85	33774	179	33775	178		1.19	1.19
4	34302.04	34284	18	34280	22		1.17	1.16
3	34465.83	34693	-227	34696	-230		1.03	1.03
2		34509		34508			0.96	0.96
4	35299.82	35162	138	35168	132		0.98	0.98
2		35504		35468			1.05	1.05
2		35790		35787			0.92	0.92
0		35856		35807				
1		36301		36271			1.11	1.10
5		36392		36392			1.12	1.12
6		37102		37088			1.08	1.08
4		37284		37234			1.24	1.24
3	37414.11	37397	17	37402	12		1.08	1.08
2		37473		37480			1.06	1.06

[a] From Kramida and Shirai (2006).

[b] Present work – model A.

[c] $\Delta E_A = E_{exp}$ - E_A.

[d] Present work – model B.

[e] $\Delta E_B = E_{exp}$ - E_B.

Table 2. Experimental and calculated energies, Landé factors and radiative lifetimes for W I odd-parity levels below 45000 cm^{-1}.

J	E_{exp}[a] (cm^{-1})	ΔE_A[b] (cm^{-1})	ΔE_B[c] (cm^{-1})	g_{exp}[a]	g_A[b]	g_B[c]	τ_{exp}[d] (ns)	τ_A[b] (ns)	τ_B[c] (ns)
0	19389.43	-1	33					5817	5411
1	20064.30	40	62	1.54	1.61	1.61	1880 ± 140	745	781
2	21448.76	-70	-55	1.48	1.49	1.49		1381	1469
1	21453.90	14	23	2.51	2.45	2.45	275 ± 14	210	221
3	23047.31	-105	-98	1.53	1.48	1.48		1310	1432
2	23964.67	7	-8	1.93	1.90	1.90	250 ± 13	172	185
4	24763.39	-54	-48	1.50	1.48	1.48	1800 ± 180	926	1017
1	25983.60	143	72	0.54	0.49	0.49	860 ± 43	1134	933
3	26189.20	45	2	1.80	1.74	1.74	161 ± 8	120	134
2	26229.77	-52	-61	1.84	1.92	2.00	76.1 ± 3.8	78.2	83.8
2	26367.28	200	226	0.87	0.81	0.72	315 ± 16	364	593
0	26629.46	-25	17					2738	3927
5	26676.48	68	83	1.46	1.47	1.47	1230 ± 80	590	642
3	27488.11	0	-15	1.72	1.72	1.72	85.6 ± 4.3	91	102
2	27662.52	-56	-77	1.21	1.22	1.23	182 ± 9	183	178
1	27778.50	-36	-54	1.25	1.28	1.28	715 ± 36	846	892
4	27889.68	74	52	1.71	1.68	1.68	59.4 ± 1.2	52.5	60.1
1	28198.90	-108	-124		2.22	2.25	132 ± 7	157	179
4	28797.24	28	19	1.61	1.57	1.56	185 ± 9	186	205
3	29139.12	-3	43	1.06	1.06	1.07	257 ± 13	306	321
2	29195.84	-31	-34	1.28	1.23	1.24	301 ± 15	453	490
2	29393.40	-75	-101	1.83	1.79	1.78	71.4 ± 3.6	69.1	75.9
6	29643.06	93	112		1.48	1.48		87290	102900
5	29773.34	104	105	1.55	1.50	1.50	695 ± 35	467	473
0	29823.09	-26	63					844	969
3	29912.85	12	-16	1.31	1.35	1.36	168 ± 8	102	101
3	30586.64	18	-2	1.64	1.55	1.54	50.2 ± 2.5	55.2	60.6
1	30683.54	13	81	1.39	1.42	1.39		1108	1068
1	31323.48	3	-67	0.86	0.90	0.91	158 ± 8	170	171
4	31432.91	-121	-84	1.32	1.31	1.30	449 ± 22	624	668
2	31817.63	31	79	1.52	1.47	1.47		619	767
3	32238.02	7	-25	1.3	1.42	1.42		379	358
0	32386.56	-92	-165					1289	1062
4	32828.12	37	12	1.7	1.22	1.23		610	546
3	32957.58	24	92	1.43	1.41	1.41		150	181
2	33141.38	50	70	1.51	1.49	1.49	115 ± 6	97	103
5	33370.04	-41	-11	1.39	1.38	1.37	439 ± 22	549	584
2	33944.06	8	-58		1.19	1.19		346	348
4	34121.68	-6	-25	1.5	1.43	1.43	188 ± 9	219	205
3	34228.60	-21	12		0.85	0.85		836	898
1	34342.44	90	123	1.56	1.56	1.55	89.9 ± 2.1	126	148
3	34354.08	-166	-149	0.71	0.84	0.82	305 ± 15	270	287
2	34485.86	-126	-165	0.82	0.90	0.88	65.9 ± 3.3	119	157
4	34632.60	71	82	0.89	0.90	0.90		396	395
1	34719.33	-126	-249	0.15	0.26	0.27	22.1 ± 0.5	24.2	24.1

Table 2. Continued.

J	$E_{exp}{}^a$ (cm^{-1})	$\Delta E_A{}^b$ (cm^{-1})	$\Delta E_B{}^c$ (cm^{-1})	$g_{exp}{}^a$	$g_A{}^b$	$g_B{}^c$	$\tau_{exp}{}^d$ (ns)	$\tau_A{}^b$ (ns)	$\tau_B{}^c$ (ns)
4	35116.78	-84	-63	1.2	1.21	1.21	83.9 ± 4.2	72.4	83.8
2	35311.56	-121	-128	1.0	0.74	0.74		108	96
3	35499.15	-37	-70	1.0	1.11	1.12	166 ± 8	226	272
5	35507.07	-29	-63		1.17	1.16		855	822
2	35731.96	-68	-127	1.5	1.53	1.52	25.7 ± 1.3	19.0	20.7
3	35943.17	33	31	1.4	1.28	1.27	282 ± 14	229	271
4	36082.30	1	23	1.24	1.25	1.25	57.9 ± 2.9	52.5	53.5
1	36190.49	124	105	1.62	1.62	1.60	18.37± 0.38	14.8	17.4
5	36275.10	43	78	1.27	1.21	1.22		180	171
0	36588.32	-71	-104					37.6	38.1
2	36673.70	43	82	1.50	1.63	1.81		16.8	10.4
3	36874.36	140	118	1.50	1.52	1.53	10.95± 0.23	8.3	8.8
2	36904.16	19	60	1.57	1.53	1.42	8.55± 0.18	7.3	12.1
4	37146.36	-22	-21	1.1	1.06	1.05	89.0 ± 4.4	92	108
5	37309.16	-25	-12	1.25	1.25	1.23	42.4 ± 2.1	37.2	48.7
6	37451.33	-30	-29		1.19	1.18		524	573
2	37466.30	-164	-187	1.28	1.17	1.14		10.3	13.1
3	37674.08	63	-3	1.13	1.13	1.11		26.1	33.8
1	37773.96	-155	-51		0.62	0.64		15.9	17.7
4	38001.12	-70	-107	1.1	1.16	1.17	111 ± 6	115	134
3	38053.05	59	126	1.11	1.20	1.24		14.7	14.6
6	38203.12	145	180		1.31	1.32		951	1182
3	38206.38	-57	-132		0.93	0.91		25.8	34.0
4	38259.40	-47	-15		1.27	1.28	16.44± 0.36	13.3	13.6
1	38355.84	104	-58		1.95	1.82	20.0 ± 0.5	14.2	11.7
0	38576.14	-46	-26					146	170
4	38748.44	43	16		1.04	1.03		22.0	27.1
2	39030.25	-45	-51		1.18	1.14	15.80± 0.34	14.2	18.6
1	39183.20	179	188	1.01	1.11	1.31	4.44 ± 0.10	3.7	5.2
5	39361.01	84	108	1.13	1.11	1.11	81.7 ± 4.0	75.5	78.8
5	39614.05	-10	4	1.20	1.14	1.14		46.4	56.7
1	39636.62	229	254	1.44	1.22	1.14	11.74± 0.25	12.1	12.0
3	39646.41	-26	-42	1.46	1.47	1.35	8.11 ± 0.21	7.3	10.3
2	39707.02	-7	-8	1.00	1.14	1.09		24.3	33.1
7	39709.04	29	54		1.24	1.24		393	485
4	39719.96	13	24	1.17	1.09	1.11	19.72± 0.76	25.1	22.6
2	40011.50	-41	-69	1.00	1.0	0.99	15.48± 0.34	14.7	16.6
4	40233.97	44	18	1.53	1.22	1.23	11.67± 0.29	14.7	16.4
3	40269.35	288	316	1.03	0.98	1.04		32.1	26.8
1	40411.12	32	-4	1.58	1.43	1.41	6.85 ± 0.15	5.9	7.1
5	40476.42	-56	-58	1.04	1.16	1.17		65.5	67.5
4	40583.07	6	-19		1.35	1.32	11.81± 0.27	5.5	7.2
3	40665.85	72	46	0.96	1.00	1.00	46.1 ± 1.0	26.5	32.2
1	40770.78	15	51	1.28	1.38	1.43	8.09 ± 0.19	8.1	8.5
2	40868.40	12	-18	1.26	1.31	1.34	7.71 ± 0.17	4.7	5.5

Table 2. Continued.

J	$E_{exp}{}^a$ (cm^{-1})	$\Delta E_A{}^b$ (cm^{-1})	$\Delta E_B{}^c$ (cm^{-1})	$g_{exp}{}^a$	$g_A{}^b$	$g_B{}^c$	$\tau_{exp}{}^d$ (ns)	$\tau_A{}^b$ (ns)	$\tau_B{}^c$ (ns)
5	40911.98	5	-16	1.03	1.14	1.14		96	102
3	40923.83	35	13	1.32	1.28	1.28		18.1	22.3
2	41104.52	31	-8	1.5	1.50	1.46		20.3	24.4
0	41127.38	77	149				10.25± 0.23	17.1	13.4
6	41171.44	151	162		1.23	1.23		146	161
4	41198.14	-68	-36	1.22	1.25	1.24		12.6	14.3
6	41417.52	-26	41	1.23	1.15	1.14		386	455
3	41499.43	23	-37	1.11	1.19	1.22	13.58± 0.41	10.2	10.6
2	41583.20	-41	35	1.06	1.38	1.43	8.53± 0.20	5.5	6.6
3	41694.34	-72	-94	1.28	1.29	1.29	14.39± 0.34	7.8	8.4
2	41734.13	46	99	1.1	1.02	1.08	12.61± 0.28	6.3	5.7
4	41871.94	8	48	1.11	1.06	1.05		45.5	60.7
0	41965.24	-6	-109					5.7	6.7
2	41978.62	135	120	0.8	0.83	0.84	12.29± 0.31	39.3	69.1
6	42239.06	82	89		1.13	1.13		253	306
3	42251.51	82	26	1.32	1.22	1.23	8.28 ± 0.18	11.2	11.5
1	42262.30	129	94	1.5	1.51	1.41		17.4	13.0
2	42449.60	-227	-258		1.21	1.21		11.4	11.9
4	42450.24	76	142		1.00	1.01		56.3	63.1
3	42514.14	40	28	1.22	1.15	1.18		23.8	35.5
4	42532.62	96	38		1.08	1.08		40.6	36.6
1	42573.49	-23	35	1.3	1.00	1.08	3.81 ± 0.11	3.4	4.0
3	42601.19	-37	-12	1.12	1.14	1.09	15.17± 0.34	20.1	21.8
5	42866.00	119	89	1.11	1.15	1.14		54.2	61.6
4	42910.74	-105	-170	1.18	1.22	1.21		13.3	14.3
5	43034.10	-14	-73		1.14	1.14	39.6 ± 0.8	42.9	44.8
0	43053.88	-202	-160					2.9	3.4
1	43217.33	17	25	1.3	0.99	1.00	9.58± 0.20	13.2	13.9
2	43227.66	58	61	1.3	1.04	1.06	7.62 ± 0.16	8.8	9.7
4	43251.00	28	-74	1.14	1.19	1.16	14.37± 0.29	16.9	23.3
7	43411.50	-171	-200	1.20	1.21	1.21		170	220
3	43478.58	96	83	1.3	1.18	1.16		11.1	14.0
2	43514.68	-128	-90	0.9	0.95	0.92		20.3	21.0
4	43720.87	12	57		1.13	1.11		37.4	32.6
5	43741.37	44	-21	1.09	1.11	1.11		94.1	93.2
3	43850.84	-106	-72	1.17	1.07	1.11	7.80 ± 0.20	6.5	7.3
1	43892.62	80	101	1.05	1.39	1.40	6.57 ± 0.24	5.6	6.2
5	43924.25	-34	-32	1.2	1.09	1.09		108	111
2	43975.22	-19	38	1.15	1.19	1.21	4.06 ± 0.12	6.0	4.8
4	43985.41	-57	2	1.24	1.12	1.13		21.7	22.1
3	44021.00	-77	-117	1.2	1.24	1.24	10.82± 0.22	9.8	9.0
1	44353.46	-27	67	1.02	1.35	1.32		4.5	5.7
2	44367.50	-13	57	1.1	1.10	1.03		9.3	13.2
6	44390.42	55	55	1.28	1.15	1.14		96	116
3	44447.02	-58	-75	1.38	1.21	1.21	8.31 ± 0.19	7.2	6.9

Table 2. Continued.

J	E_{exp}[a] (cm^{-1})	ΔE_A[b] (cm^{-1})	ΔE_B[c] (cm^{-1})	g_{exp}[a]	g_A[b]	g_B[c]	τ_{exp}[d] (ns)	τ_A[b] (ns)	τ_B[c] (ns)
5	44546.76	-145	-129	1.3	1.20	1.17		14.0	18.2
2	44596.28	53	43	1.11	1.37	1.39		10.0	18.7
1	44737.21	-51	103		0.90	0.92		10.2	9.6
6	44923.90	-31	-19		1.20	1.20		30.0	29.6
4	44940.57	-92	-36		1.11	1.12		24.0	24.6
7	44970.82	82	80		1.20	1.20		75.9	77.1

[a] From Wyart (2010).
[b] Present work – model A ($\Delta E_A = E_{exp}$ - E_A).
[c] Present work – model B ($\Delta E_B = E_{exp}$ - E_B).
[d] From Den Hartog *et al* (1987) and Schnabel and Kock (1997).

Table 3. Radiative transition probabilities for atomic tungsten lines. Only the most intense transitions ($gA_{calc} \geq 5 \times 10^7$ s^{-1}) are listed in the table.

λ^a (nm)	E^b_{Low} (cm^{-1})	J	$E^b_{Upp.}$ (cm^{-1})	J'	Int.^{b}	gA^c_{exp1} (10^8 s^{-1})	gA^d_{exp2} (10^8 s^{-1})	gA^e_A (10^8 s^{-1})	gA^f_B (10^8 s^{-1})
225.391	0.00	0	44353.46	1	25			1.18	0.95
227.7583	0.00	0	43892.62	1	60		1.86 (0.21)	2.38	2.10
231.3170	0.00	0	43217.33	1	30		1.47 (0.18)	1.09	0.97
232.8872	1670.29	1	44596.28	2	15			0.77	0.23
236.3072	1670.29	1	43975.22	2	18		3.45 (0.35)	3.75	3.58
236.7693	1670.29	1	43892.62	1	10		0.70 (0.09)	0.79	0.62
238.9078	1670.29	1	43514.68	2	15			0.75	0.16
240.5580	1670.29	1	43227.66	2	30		3.45 (0.35)	2.79	2.67
241.4039	3325.53	2	44737.21	1	20			0.79	0.99
241.5685	1670.29	1	43053.88	0	35			3.36	2.82
242.2292	3325.53	2	44596.28	2	30			1.65	0.50
243.1081	3325.53	2	44447.02	3	25		2.01 (0.21)	3.72	6.01
243.5782	3325.53	2	44367.50	2	12			1.89	1.03
243.6624	3325.53	2	44353.46	1	25			4.02	2.94
244.4056	1670.29	1	42573.49	1	60		2.62 (0.16)	3.01	2.18
245.1484	1670.29	1	42449.60	2	70			2.86	2.77
245.1996	0.00	0	40770.78	1	100		2.34 (0.23)	1.16	0.91
245.6534	3325.53	2	44021.00	3	150		3.30 (0.28)	1.43	1.10
245.9300	3325.53	2	43975.22	2	140		4.31 (0.43)	2.66	3.65
246.2793	1670.29	1	42262.30	1	100			0.97	1.45
246.4305	3325.53	2	43892.62	1	60		1.29 (0.15)	1.41	1.17
246.6848	3325.53	2	43850.84	3	100		4.52 (0.35)	7.38	6.53
248.0130	1670.29	1	41978.62	2	100		2.35 (0.25)	0.59	0.04
248.0955	1670.29	1	41965.24	0	60			1.55	1.32
248.9720	3325.53	2	43478.58	3	35			4.29	3.38
249.5264	1670.29	1	41734.13	2	100		2.33 (0.23)	3.20	4.70
250.4698	1670.29	1	41583.20	2	60		1.58 (0.18)	4.80	3.41
251.3934	4830.00	3	44596.28	2	30			1.17	0.65
252.3410	4830.00	3	44447.02	3	60		3.59 (0.39)	2.24	1.11
252.8486	4830.00	3	44367.50	2	50			2.80	1.94
253.3635	1670.29	1	41127.38	0	30		0.98 (0.07)	0.52	0.70
254.5340	3325.53	2	42601.19	3	50		1.69 (0.14)	1.19	1.05
254.7136	3325.53	2	42573.49	1	100		5.25 (0.30)	4.61	4.49
255.0378	1670.29	1	40868.40	2	60		1.40 (0.15)	2.19	1.44
255.0843	4830.00	3	44021.00	3	4			3.16	4.67
255.100	3325.53	2	42514.14	3	25			0.78	0.42
255.1349	0.00	0	39183.20	1	200		5.34 (0.45)	7.51	5.44
255.3824	4830.00	3	43975.22	2	100		2.13 (0.20)	0.92	2.35
255.5207	3325.53	2	42449.60	2	40			0.66	0.58
255.6749	1670.29	1	40770.78	1	40		0.79 (0.08)	1.81	1.93
256.1968	4830.00	3	43850.84	3	100		3.35 (0.28)	0.95	0.32
256.8214	3325.53	2	42251.51	3	30		0.23 (0.02)	0.61	0.74
258.0337	2951.29	3	41694.34	3	30		0.73 (0.11)	1.86	1.77
258.0487	1670.29	1	40411.12	1	125		2.25 (0.15)	3.37	2.81
260.2804	3325.53	2	41734.13	2	25		0.47 (0.05)	3.29	2.75

Table 3. Continued.

λ^a (nm)	E^b_{Low} (cm^{-1})	J	$E^b_{Upp.}$ (cm^{-1})	J'	Int.^{b}	gA^c_{exp1} (10^8 s^{-1})	gA^d_{exp2} (10^8 s^{-1})	gA^e_A (10^8 s^{-1})	gA^f_B (10^8 s^{-1})
260.3544	4830.00	3	43227.66	2	40		1.41 (0.15)	1.81	1.64
260.6388	0.00	0	38355.84	1	35			1.63	2.15
260.7378	1670.29	1	40011.50	2	35		0.60 (0.04)	1.01	0.99
260.832	6219.33	4	44546.76	5	50			3.71	2.54
261.3076	3325.53	2	41583.20	2	80		2.70 (0.30)	0.55	0.84
261.3818	2951.29	3	41198.14	4	50			3.85	3.29
261.5124	6219.33	4	44447.02	3	40		1.11 (0.13)	1.68	1.26
262.0215	2951.29	3	41104.52	2	50			0.90	0.64
262.5220	4830.00	3	42910.74	4	60			3.72	3.01
262.8255	1670.29	1	39707.02	2	40			0.90	0.67
263.2695	2951.29	3	40923.83	3	80			2.13	1.81
263.3129	1670.29	1	39636.62	1	150		1.96 (0.15)	1.66	1.54
264.6185	3325.53	2	41104.52	2	70			1.26	1.10
264.6536	0.00	0	37773.96	1	15			0.54	0.59
264.6730	4830.00	3	42601.19	3	80		1.08 (0.08)	0.65	0.50
264.7091	6219.33	4	43985.41	4	60			0.89	1.02
265.1546	4830.00	3	42532.62	4	5			0.80	0.90
265.2844	4830.00	3	42514.14	3	8			0.89	0.63
265.6540	2951.29	3	40583.07	4	300		6.07 (0.41)	15.90	12.10
265.7361	4830.00	3	42450.24	4	60			1.14	0.94
266.2835	3325.53	2	40868.40	2	200		2.11 (0.15)	5.00	4.21
267.1472	4830.00	3	42251.51	3	200		2.74 (0.25)	3.60	3.40
267.7276	3325.53	2	40665.85	3	100		1.11 (0.08)	1.60	1.31
267.8878	2951.29	3	40269.35	3	150			0.61	1.18
268.1422	2951.29	3	40233.97	4	400		6.62 (0.45)	5.16	4.66
269.567	3325.53	2	40411.12	1	150		1.41 (0.12)	0.94	0.80
269.9594	6219.33	4	43251.00	4	150		3.42 (0.27)	2.64	1.32
270.8927	4830.00	3	41734.13	2	80			0.71	0.78
271.1846	4830.00	3	41694.34	3	8			0.85	0.81
271.5503	6219.33	4	43034.10	5	75		1.53 (0.11)	0.76	0.96
271.8906	2951.29	3	39719.96	4	250		4.26 (0.27)	3.11	3.47
272.0046	4830.00	3	41583.20	2	30			1.74	1.18
272.4352	2951.29	3	39646.41	3	300		7.35 (0.56)	8.74	5.86
272.4624	6219.33	4	42910.74	4	35			1.85	2.56
272.7954	6219.33	4	42866.00	5	40			1.30	1.12
274.8844	4830.00	3	41198.14	4	80			2.42	2.30
276.8982	1670.29	1	37773.96	1	100			1.21	0.98
276.9741	4830.00	3	40923.83	3	80			0.93	0.76
277.0880	2951.29	3	39030.25	2	200		0.92 (0.08)	1.32	0.97
277.3999	4830.00	3	40868.40	2	200		1.96 (0.15)	2.03	2.24
277.4476	6219.33	4	42251.51	3	300		3.33 (0.28)	1.14	1.10
279.2696	2951.29	3	38748.44	4	60			1.57	1.17
279.9928	3325.53	2	39030.25	2	50		0.65 (0.05)	0.62	0.51
281.8060	6219.33	4	41694.34	3	250		3.02 (0.28)	4.43	3.91
283.1379	2951.29	3	38259.40	4	250		4.42 (0.36)	5.91	5.41

Table 3. Continued.

λ^a (nm)	E^b_{Low} (cm^{-1})	J	$E^b_{Upp.}$ (cm^{-1})	J'	Int.^{b}	gA^c_{exp1} (10^8 s^{-1})	gA^d_{exp2} (10^8 s^{-1})	gA^e_A (10^8 s^{-1})	gA^f_B (10^8 s^{-1})
283.3630	6219.33	4	41499.43	3	120		3.35 (0.25)	4.21	4.16
283.9340	9528.06	0	44737.21	1	50			0.79	0.78
284.1570	4830.00	3	40011.50	2	80		0.87 (0.06)	1.01	0.90
284.8022	2951.29	3	38053.05	3	180			2.98	2.91
285.6030	1670.29	1	36674.08	2	150			0.92	0.32
286.6062	3325.53	2	38206.38	3	200			1.60	1.18
287.8721	3325.53	2	38053.05	3	50			1.08	1.31
287.9112	2951.29	3	37674.08	3	150			1.46	1.04
287.9396	0.00	0	34719.33	1	140	0.73 (0.09)	0.74 (0.05)	0.91	0.95
288.1606	6219.33	4	40911.98	5	80			0.69	0.71
289.6009	1670.29	1	36190.49	1	150		0.84 (0.05)	0.85	0.77
289.6442	2951.29	3	37466.30	2	400			4.04	3.09
291.8254	6219.33	4	40476.42	5	100			1.12	1.17
292.3103	4830.00	3	39030.25	2	150		0.38 (0.03)	0.50	0.33
293.4996	1670.29	1	35731.96	2	250	0.73 (0.08)		0.97	0.93
294.4398	2951.29	3	36904.16	2	300		5.40 (0.40)	6.24	3.00
294.6989	2951.29	3	36874.36	3	300		5.76 (0.42)	7.01	6.69
294.7388	4830.00	3	38748.44	4	150			2.03	1.79
296.4520	2951.29	3	36673.70	2	150			1.77	4.36
297.9860	3325.53	2	36874.36	3	70			1.08	0.96
299.3614	6219.33	4	39614.05	5	125			1.96	1.54
301.3788	4830.00	3	38001.12	4	120	0.58 (0.04)		0.51	0.20
301.6466	6219.33	4	39361.01	5	150	1.02 (0.06)		0.86	0.88
301.7436	2951.29	3	36082.30	4	200	1.09 (0.07)		1.18	1.29
302.5263	9528.06	0	42573.49	1	50			0.64	0.46
304.1863	3325.53	2	36190.49	1	80			0.63	0.53
304.9688	2951.29	3	35731.96	2	120	0.86 (0.07)		1.28	1.12
321.5562	6219.33	4	37309.16	5	200	2.30 (0.10)		2.70	2.04
330.0822	4830.00	3	35116.78	4	150	0.73 (0.05)		0.73	0.57
339.1520	15069.93	5	44546.76	5	80			0.52	0.53
353.7446	15460.01	3	43720.87	4	80			0.53	0.58
357.5220	17008.50	6	44970.82	7	80			1.24	1.15
361.7515	2951.29	3	30586.64	3	500	0.75 (0.04)		0.65	0.59
365.0997	17008.50	6	44390.42	6	60			0.61	0.56
377.3706	13777.71	2	40269.35	3	150			0.68	0.59
381.0380	18116.84	2	44353.46	1	100			0.61	0.51
394.7977	19648.54	6	44970.82	7	20			0.69	0.76
395.5304	19648.54	6	44923.90	6	40			1.16	1.09
396.8590	19256.24	4	44447.02	3	20		0.65 (0.07)	0.83	0.62
398.3292	19826.04	5	44923.90	6	50			2.88	2.97
400.8753	2951.29	3	27889.68	4	1000	1.47 (0.07)	1.50 (0.11)	1.65	1.43
401.5218	19648.54	6	44546.76	5	100			2.46	1.76
403.6855	19256.24	4	44021.00	3	40		1.04 (0.07)	0.85	0.42
407.4358	2951.29	3	27488.11	3	600	0.73 (0.04)		0.68	0.61
411.8052	18974.51	3	43251.00	4	25		0.83 (0.06)	0.51	0.25

Table 3. Continued.

λ^a (nm)	E^b_{Low} (cm^{-1})	J	$E^b_{Upp.}$ (cm^{-1})	J'	Int.^{b}	gA^c_{exp1} (10^8 s^{-1})	gA^d_{exp2} (10^8 s^{-1})	gA^e_A (10^8 s^{-1})	gA^f_B (10^8 s^{-1})
413.8018	19826.04	5	43985.41	4	40			0.60	0.51
420.4405	19256.24	4	43034.10	5	30		0.57 (0.04)	0.98	0.83
420.7052	19648.54	6	43411.50	7	50			0.77	0.60
427.5486	18116.84	2	41499.43	3	50		0.65 (0.05)	0.79	0.78
429.4606	2951.29	3	26229.77	2	800	0.62 (0.03)	0.62 (0.02)	0.61	0.56

[a] Observed air wavelengths taken from Kramida and Shirai (2006).

[b] From Kramida and Shirai (2006).

[c] From Den Hartog *et al* (1987). Absolute uncertainties are given in parentheses.

[d] From Kling and Kock (1999). Absolute uncertainties are given in parentheses.

[e] Present work – model A.

[f] Present work – model B.

$A(B)$ stands for $A \times 10^B$.